

THE EFFECT OF TWO-DIMENSIONAL PHENOMENA ON THE BUNCHING OF INTENSE ELECTRON BEAMS IN BROADBAND KLYSTRONS

© 2025 V. E. Rodyakin^{a,*}, V. N. Aksenov^b

^a*Institute on Laser and Information Technologies of Russian Academy of Sciences,
National Research Centre “Kurchatov Institute”, Shatura, Russia*

^b*Lomonosov Moscow State University, Moscow, Russia*

*e-mail: vrodyakin@mail.ru

Received September 06, 2024

Revised September 16, 2024

Accepted September 30, 2024

Abstract. The results of a study of the effect of two-dimensional phenomena on the electron beam bunching in single-beam and multi-beam broadband klystrons are presented. The results of a comparative analysis of beam bunching using a one-dimensional and two-dimensional model are presented. The causes of errors in determining the output parameters of broadband klystrons obtained using one-dimensional programs are analyzed.

Keywords: *electron beam, broadband klystron, amplifier, electron grouping, velocity modulation, multibeam klystron*

DOI: 10.31857/S03676765250116e7

INTRODUCTION

The development and creation of powerful broadband amplifying klystrons remains a very urgent task. Currently, klystrons with a bandwidth from 2 to 15% are widely used in transmitters of powerful radars for various purposes in the decimeter,

centimeter and millimeter wave ranges. In its basis, a klystron is a resonant narrow-band device of "O" type with discrete interaction of electron flux with electromagnetic fields of resonators and with a gain bandwidth of less than 1%.

To extend the operating bandwidth of the klystron, low-frequency intermediate resonators are used, with relatively strong frequency detuning from the center frequency of the amplifier operating range. The first few intermediate resonators are usually tuned to frequencies within the operating band and form a linear amplifier, which forms the bandwidth of amplified frequencies and the required gain level. Subsequent intermediate resonators are tuned to frequencies beyond the right bandwidth and form a nonlinear grouper responsible for obtaining high efficiency of the klystron and correcting its bandwidth response.

In addition to expanding the "natural gain bandwidth of the klystron by tuning the intermediate resonators, it is important for broadband klystrons that the output system also has a wide bandwidth. For this purpose, it is necessary to reduce its loaded goodness, which, in turn, increases the active component of the conductance of the output resonator system. To ensure efficient energy extraction in the output system, it is necessary that the conductance of the electron flux is approximately equal to the conductance of the output system. Therefore, either high-perveance electron beams or multibeam designs are used to increase the electron flux conductance. In addition, multigap resonators are used as output systems of broadband devices to widen the bandwidth.

All these factors complicate physical processes in klystrons and require system two-dimensional and three-dimensional numerical analysis when developing their

design. Application of one-dimensional programs for optimization of parameters of structural elements of broadband klystrons is limited by the initial stage of research of processes in such devices. The limits of applicability of analytical and one-dimensional numerical models for description of nonlinear processes in klystrons were shown in [1, 2]. There were also given estimates of the influence on the grouping efficiency from the transverse beam stratification caused by radial inhomogeneity of the space charge forces, potential sag, and radial inhomogeneity of the resonator fields.

This paper considers the peculiarities of the influence of these two-dimensional factors on the grouping efficiency in broadband klystrons on the example of single-beam and multibeam klystrons. Since the influence on efficiency of electron beam grouping of various nonlinear factors occurs simultaneously, it is difficult to determine the degree of influence of each factor separately. Therefore, to investigate their influence, we will use the results of a comparative analysis of the grouping efficiency by different physical models.

RESEARCH METHODS

The theory of powerful electrovacuum microwave devices is generally based on the principles of classical electrodynamics and is reduced to the solution of the joint system of Maxwell's equations and the equations of motion of charged particles. The direct solution of this system in the general formulation requires the use of nonstationary three-dimensional numerical models of electron flow and electromagnetic fields. Such a solution is very labor-intensive, requires significant

computational costs, and is applied only in complete computer codes such as CST Studio Suite [3].

When analyzing the processes of grouping and energy extraction in klystrons in the two-dimensional approximation, we used the PARS software package [4], developed by the authors on the basis of an upgrade of the Arsenal-MGU program [5], which proved to be a reliable tool for the development of numerous klystron amplifiers in our country and abroad [6-9]. [5], which has proved itself in our country and abroad as a reliable tool for the development and research of numerous klystron amplifiers [6-9]. In the model, the electron beam is represented by a sequence of charged rings whose motion takes into account the longitudinal and radial coordinates, as well as all three velocity components.

The program "Klystron - MSU" was used to perform comparative calculations in one-dimensional approximation [10], which was successfully used in the development of numerous klystrons in the USSR. In the model, the electron beam is represented as a sequence of charged disks whose motion takes into account only the longitudinal coordinate and the longitudinal velocity component.

In addition to the difference in the electron beam models, the programs differ in their approaches to calculating the amplitudes of the voltages arising in the resonator gaps. In the one-dimensional program "Klystron - MSU", the static complex conductivity of the electron beam $G_{en} + iB_{en}$ is introduced in the equivalent circuit of the resonator, which is calculated by analytical formulas assuming that the electron beam entering the resonator is unmodulated. To find the voltage amplitude at the resonator gap, a linear approximation is used, which allows one to calculate the value of the

induced current from the known value of the first harmonic of the convection current $I_{(1)(n)}$ at the center of the resonator gap:

$$I_{\text{hab n}} = M_n I_{1n}, \quad (1)$$

where M_n is the electron interaction coefficient of the n -th resonator gap. The voltage amplitude at the gap of the n -th resonator in the linear approximation is determined from the following expression:

$$V_n = \frac{I_{\text{hab n}}}{\sqrt{(G_{cn} + G_{en})^2 + (B_{cn} + B_{en})^2}}, \quad (2)$$

where $B_{cn} = \frac{1}{\rho_n} \left[1 - \left(\frac{\omega_0}{\omega} \right)^2 \right]$ is the reactive conductance of the resonator, $G_{cn} = \frac{1}{\rho_n Q_n}$

is the active conductance of the resonator, where $\omega_n = 2\pi f_n Q_n \rho_n f_n$, ω is the eigenvalue, wave impedance and natural frequency of the working mode of the resonator.

In the two-dimensional PARS program, a nonlinear approach is already used to calculate the voltage amplitude at the gap of the intermediate resonator using the Shockley-Ramo theory, and the voltage at the resonator gap is determined by an iterative method through the interaction power:

$$P(t) = \int_{V_{gn}} \vec{E}_{gn} \cdot \vec{J} dV_{gn}, \quad (3)$$

where V_{gn} is the volume of the interaction region of the electric field of the n -th resonator \vec{E}_{gn} with the electron beam, \vec{J} is the vector of the beam convection current density. At the same time, at each period of field oscillations in the resonator $T = \frac{1}{f}$ the real and imaginary parts of the complex induced current are calculated:

$$\text{Re } \vec{I}_{\text{hab n}} = \frac{2}{T_{dn}} \int_0^T dt \iiint_{V_{gn}} [j_r(r, z, t) F_{rn}(r, z) + j_z(r, z, t) F_{zn}(r, z)] \sin(\omega t + \alpha_n) dV_{gn} \quad (4)$$

$$\text{Im } \vec{I}_{\text{HAB n}} = \frac{2}{T_{dn}} \int_0^T dt \iiint_{V_{gn}} [j_r(r, z, t) F_{rn}(r, z) + j_z(r, z, t) F_{zn}(r, z)] \cos(\omega t + \alpha_n) dV_{gn}, \quad (5)$$

where, $F_{rn}(r, z)$ $F_{zn}(r, z)$ are the distribution functions of the radial and longitudinal components of the intrinsic electric field of the n-th resonator. The amplitude and phase of the voltage at k+1 period (iteration) are determined from the following expression:

$$\vec{V}_n^{k+1} = \sqrt{\frac{\vec{I}_{\text{HAB n}} \vec{V}_n^k}{(G_{cn} + iB_{cn})}} \quad (6)$$

The iterations continue until the amplitude and phase of the voltage at the resonator gap converge to a stationary value. The developed nonlinear method of analysis makes it possible to take into account in the quasi-stationary quasi-tree-dimensional approximation the nonlinear effects of interaction of intense electron fluxes with electromagnetic fields in the gaps of resonators, including the output ones.

RESEARCH RESULTS

Two broadband C-band pulse amplifier klystrons developed by the specialists of the Institute of Electronics of the Chinese Academy of Sciences (IECAS) using the one-dimensional program KLY6 were investigated. The parameters of the fabricated devices are summarized in Table 1. The KC4083A klystron is a single-beam klystron and utilizes a high-perveance electron beam. The coupling system of the klystron consists of nine resonators, the last of which is a double-gap output resonator operating on π -type oscillations. The parameters of the KC4083A klystron resonators are listed in Table 2. The KC4079E klystron is a multi-beam klystron and utilizes a low perveance electron beam. The interaction system of the klystron consists of seven resonators, the last of which is a double-gap output resonator operating on a 2π -type of oscillation. The resonator parameters of the KC4079E klystron are listed in Table 3.

Both klystrons use a scheme with frequency detuning of the second resonator in the left part of the gain bandwidth.

When testing both klystrons, IECAS specialists faced a very unpleasant problem. The amplitude-frequency characteristics (AFR) of the fabricated devices had very significant dips near of the center frequency of the gain band (curves 1 in Fig. 1). At the request of Chinese specialists, theoretical studies of the operation of the fabricated klystrons were carried out using the programs Klystron-MGU and Arsenal-MGU.

Studies using the one-dimensional Klystron-MGU program (curves 3 in Fig.1) did not show the presence of dips. This corresponds to the results obtained by IECAS specialists using the one-dimensional program KLY6 (curve 4 in Fig.1). The results obtained with the two-dimensional Arsenal-MSU program (curves 2 in Fig.1) coincided very well with the experimental results [11].

In order to understand the reasons for such a difference between the analysis results obtained by one-dimensional and two-dimensional programs, a more detailed study of physical processes in the KC4083A and KC4079E klystrons was carried out using the one-dimensional Klystron-MSU program and the two-dimensional PARS program.

Figures 2a and 2b show the instantaneous values of the relative longitudinal components of the charged particle pulses and their positions calculated by the PARS program for the KC4083A klystron, respectively. These results were obtained for the frequency of the input signal having a detuning from the center frequency of the gain band $\Delta f = -20$ MHz. As can be seen from the figures, the beam electrons are velocity modulated by the electromagnetic field of the input resonator. Modulation in velocity

leads to modulation in density and grouping of electrons into clots. The electromagnetic fields of the subsequent intermediate resonators, excited by the clots of electrons, enhance the modulation in velocity and density. The degree of electron compression in the clots is characterized by the amplitude of the first harmonic of the convection current I_1 , which gradually increases along the length of the device.

One of the main features of broadband klystrons is the strong dependence of the rise character $I_{(1)}(Z)$ on the frequency of the input signal. Figure 2c shows the calculated longitudinal distributions of the relative first harmonic of the convection current in the device for different values of the input signal frequency detuning Δf . Due to the second and third resonators of the klystron linear amplifier, whose frequencies are detuned to the left of the center frequency, the amplitude buildup $I_{(1)}(Z)$ for the frequencies of the left edge of the band is more uniform than at the right edge. The grouping at the right edge of the band is non-uniform along the length of the device and occurs mainly due to the effective interaction with the fields of the resonators of the nonlinear grouper. In this case, significant voltage amplitudes appear at their gaps.

The two-dimensional PARS program was used to study the effect of dynamic defocusing of the electron beam on the AFC of the device. The results were compared for the case of using experimental data for a focusing magnetic field and for the case of a "frozen" beam with an infinite magnetic field, in which there are no radial pulsations of electrons in the beam. The comparison showed a weak influence on the AFC from the dynamic defocusing in this klystron.

In Figure 2c, the distribution of $I_{(1)}(Z)$ corresponding to the frequency detuning of the AFC dip $\Delta f = 40$ MHz (Figure 2a) is labeled with number 6. It can be observed that

the low value of I_1 at the end of the grouper is caused by the weak beam grouping by the resonators of the KC4083A klystron linear amplifier. Therefore, a section of the KC4083A klystron including the first five resonators was chosen for a detailed comparative analysis of the grouping process. A "frozen" electron beam was used in the PARS program calculations. The results of the analysis for the frequency $\Delta f = 40$ MHz are shown in Figure 3. The dotted lines mark the positions of the resonator centers. The shaded areas correspond to the zones of interaction between the electromagnetic fields of the resonators and the electron flux. In these areas, the integral values of the interaction power are calculated in the two-dimensional PARS program.

Figure 3a shows the longitudinal distributions of $I_{(1)}(z)$ calculated from the one-dimensional model (curve 1) and the two-dimensional model (curve 2). The course of curves 1 and 2 coincide up to the third resonator. The voltage amplitude at the third resonator obtained with the two-dimensional program coincides with the amplitude calculated from the one-dimensional model. However, the voltage phase calculated using the two-dimensional program is very different from the phase determined using the one-dimensional Klystron-MGU program. The reasons for this can be understood from Figure 3b, which shows the longitudinal distributions of the longitudinal component of the relative first harmonic of the convection current for different radial layers of the electron beam. It follows from the figure that in the grouping of different layers is noticeably different already in the second resonator, while in the third resonator electrons of different layers enter in different phases. The electrons of the outer layers continue to demodulate after the demodulating effect of the fields of the

second resonator, which is tuned below the signal frequency. The electrons of the inner layers have already finished demodulating and start to modulate again. As a result, the phase shift between the nonlinear conductivity of the third resonator and the convection current has the opposite sign to the phase shift between the linear conductivity and the convection current. This leads to a marked difference in the phase of the third resonator voltage and, as a consequence, to different behavior of electrons in the beam. This can be clearly seen in Figure 3a, where the curve $I_{(1)}(Z)$ calculated with the one-dimensional program starts its rise again, while the curve obtained with the two-dimensional program continues its fall after the third resonator. As a consequence, the amplitude I_1 at the fourth resonator, calculated by the two-dimensional program is 4 times smaller than that determined by the one-dimensional model. During further amplification, the error of the one-dimensional program in determining the voltage at the third resonator leads to a very significant accumulated error in determining the output power at this frequency. Thus, the failure to account for two-dimensional stratification of the high-perveance electron beam in the one-dimensional models resulted in noticeable errors in the AFC of the KC4083A single-beam klystron.

For a detailed comparative analysis of the grouping process in the KC4079E multibeam klystron, a section of the klystron, including the first four resonators, was selected. A "frozen" electron beam was used in the PARS program calculations. The results of the analysis for the center frequency ($\Delta f = 0$ MHz) are shown in Figure 4.

Figure 4a shows the longitudinal distributions of $I_{(1)}(Z)$ calculated from the one-dimensional model (curve 1) and the two-dimensional model (curve 2). The course of curves 1 and 2 coincide up to the third resonator. Due to the fact that the device uses

an electron beam with a low perveance value, no stratification effect was observed in the PARS calculations. Therefore, the voltage phase at the third resonator obtained with the two-dimensional program coincides with the phase calculated from the one-dimensional model. However, the voltage amplitude calculated using the two-dimensional program differs from the amplitude determined using the one-dimensional Klystron-MGU program by 40%. The reasons for this can be understood from Figure 4b, which shows the dependences of the relative impedance of the third resonator calculated by the linear model (curve 1 in Fig. 4b) and by the nonlinear model (curve 2 in Fig. 4b).

The figure shows that in the region of resonance with the natural frequency of the third resonator, there is a 40% drop in the amplitude of the impedance of the third resonator, which leads to a corresponding decrease in the amplitude of the voltage on the third resonator. During further amplification, the error of the one-dimensional program in determining the voltage at the third resonator results in a very significant accumulated error in determining the output power at this frequency. Thus, incorrect accounting of the total conductivity of the resonator near resonance in one-dimensional models led to noticeable errors in the AFC of the KC4079E multibeam klystron with a low-perveance electron beam.

CONCLUSION

As a result of the studies, it was found that when modeling the grouping of intense electron fluxes with a high value of perveance in broadband klystrons using one-dimensional computer programs at some points of the band, a significant error in determining the output parameters of the device can occur. The error is caused by the

lack of consideration in one-dimensional models of the effect of electron beam stratification.

The comparative analysis of grouping in a broadband multibeam klystron using one-dimensional and two-dimensional programs has shown the possibility of obtaining incorrect characteristics of the device when using one-dimensional models, caused by incorrect accounting for the electronic conductivity of the beam. At the points of the gain bandwidth near the resonance frequencies of the resonators of the linear amplifier, it is possible to reduce the total impedance of the resonators due to the influence of electron fluxes and, as a consequence, to reduce the output parameters of the amplifier.

In the design of wideband klystron amplifiers, one should be cautious when using one-dimensional programs to optimize the devices in the frequency band. The final results should be verified with two-dimensional and three-dimensional models.

FUNDING

The work was carried out within the framework of fulfillment of the state assignment of SIC "Kurchatov Institute".

REFERENCES

1. *Rodyakin V.E., Pikunov V.M., Aksenov V.N.* // J. Radio Electron. 2020. No. 12. Art. No. 14.
2. *Rodyakin V.E., Aksenov V.N.* // Vest. Mosk. un-ta. Ser. 3. Phys. Astron. 2021. № 5. C. 70.
3. www.cst.com.
4. *Rodyakin V.E., Pikunov V.M., Aksenov V.N.* // J. Radio Electron. 2019. No. 6. Art. No. 4.
5. *Sandalov A.N., Pikunov V.M., Rodyakin V.E. et al.* // KEK report 1/1997. P. 185.

6. *Shen B., Ding Y., Zhang Z. et al. // IEEE Trans. Electron Devices. 2014. V. 61. No. 6. P. 1848.*
7. *Zhiqiang Zhang, Jirun Luo, Zhaochuan Zhang et al. // Progr. Electromagn. Res. C. 2020. V. 103. P. 177.*
8. *Rodyakin V.E., Pikunov V.M., Aksenov V.N. // Bull. Russ. Acad. Sci. 2021. V. 85. No. 1. P. 83.*
9. *Rodyakin V.E., Aksenov V.N. // Bull. Russ. Acad. Sci. 2022. V. 86. No. 1. P. 62.*
10. *Kanavets V.I., Sandalov A.N. // Electron. tehn. ser. 1. Microwave Electronics. 1971. № 3. C.11.*
11. *Ding Y., Yunshu Zhu, Xiuling Yin et al. // IEEE Trans. Electron Devices. 2007. V. 54. No. 4. P. 624.*

FIGURE CAPTIONS

Fig. 1. AFCs of KC4083A (a) and KC4079E(b) klystrons obtained in the experiment (curve 1), using the two-dimensional program "Arsenal-MSU" (curve 2), using the one-dimensional programs "Klystron-MSU" (curve 3) and KLY6 (curve 4).

Fig. 2. Instantaneous values of relative longitudinal components of charged particle pulses (a), their positions (b) and longitudinal distributions of the relative first harmonic of the convection current in the device calculated by the PARS program for the KC4083A klystron for different values of the input signal frequency detuning from the center frequency of the device operating band Δf , MHz: -180 (1), -40 (2), -20 (3), 0 (4), 20 (5), 40 (6), 60 (7), 100 (8), 160 (9)..

Fig. 3. Longitudinal dependences of the relative first harmonic of the convection current obtained for the KC4083A klystron using the one-dimensional Klystron-MSU program (curve 1 in Fig. 3a) and the two-dimensional Arsenal-MSU program (curve 2

in Fig. 3a), as well as longitudinal distributions of the relative amplitude of the first harmonic of the convection current calculated using the two-dimensional Arsenal-MSU program in different radial layers of the electron beam (Fig. 3b).

Fig. 4. Longitudinal dependences of the relative first harmonic of the convection current obtained for the KC4079E klystron, using the one-dimensional program "Klystron-MSU" (curve 1 in Fig. 4a) and the two-dimensional program "Arsenal-MSU" (curve 2 in Fig. 4a), as well as dependences of the relative impedance of the third resonator calculated by the linear model (curve 1 in Fig. 4b) and by the nonlinear model (curve 2 in Fig. 4b).

Table 1. Parameters of klystrons.

Parameter	KC4083A	KC4079E
Boost voltage, kV	68.2	23
Current force per beam, A	39.2	1.2
Microperveance, $\mu\text{A}/\text{V}^{3/2}$	2.2	0.344
Pipe radius, cm	0.43	0.175
Number of rays	1	24
Beam radius, cm	0.32	0.105
EFFICIENCY	30%	30%
Band width	7%	5.3%
Gain, dB	45	35
Output power, kW	800	200

Table 2. Parameters of the KC4083A klystron resonators

№	$z, \text{ cm}$	f/f_0	ρOhm	Q
1	0	0.9866	100	50
2	3.4	0.9671	110	230
3	7.2	0.9971	110	120
4	10.2	1.0199	110	67
5	13.4	1.0368	110	105
6	16.6	1.046	110	210
7	19.6	1.0575	110	180
8	22	1.0699	110	3000
9	24.3	1	67.5	138

Table 3. Parameters of the KC4079E klystron resonators

№	$z, \text{ cm}$	f/f_0	ρOhm	Q
1	0	0.991935	22	65
2	3.2	0.967742	22	250
3	6.4	1.005376	22	150
4	9.6	1.016129	22	150
5	12.8	1.031362	22	500
6	16.2	1.039427	22	500
7	17.8	1	20	30

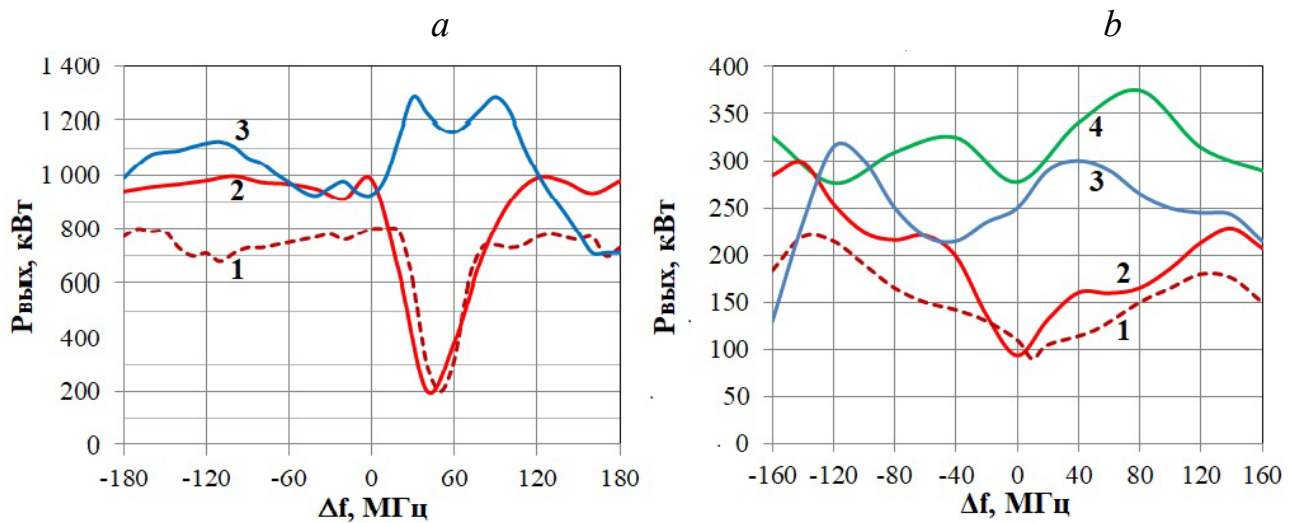


Fig. 1.

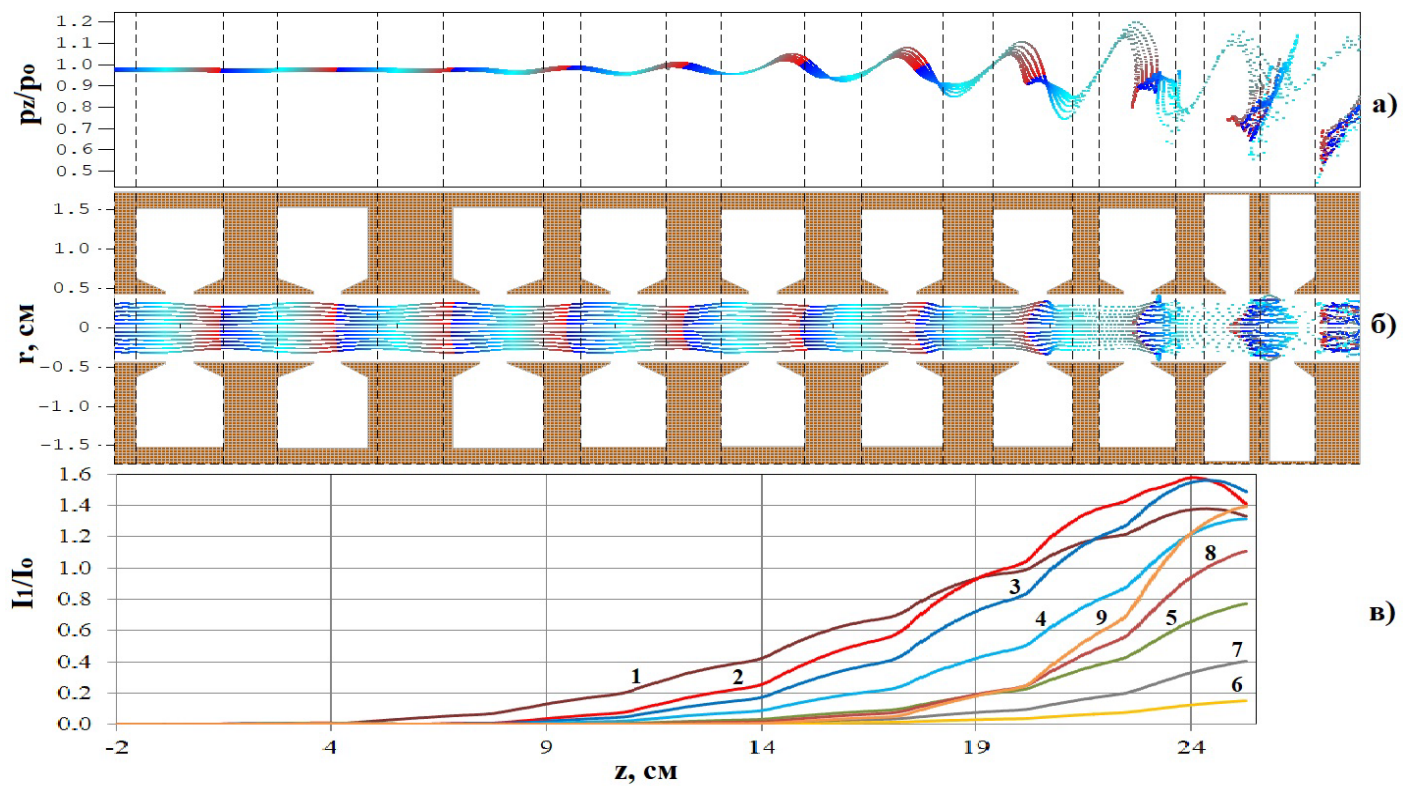


Fig. 2.

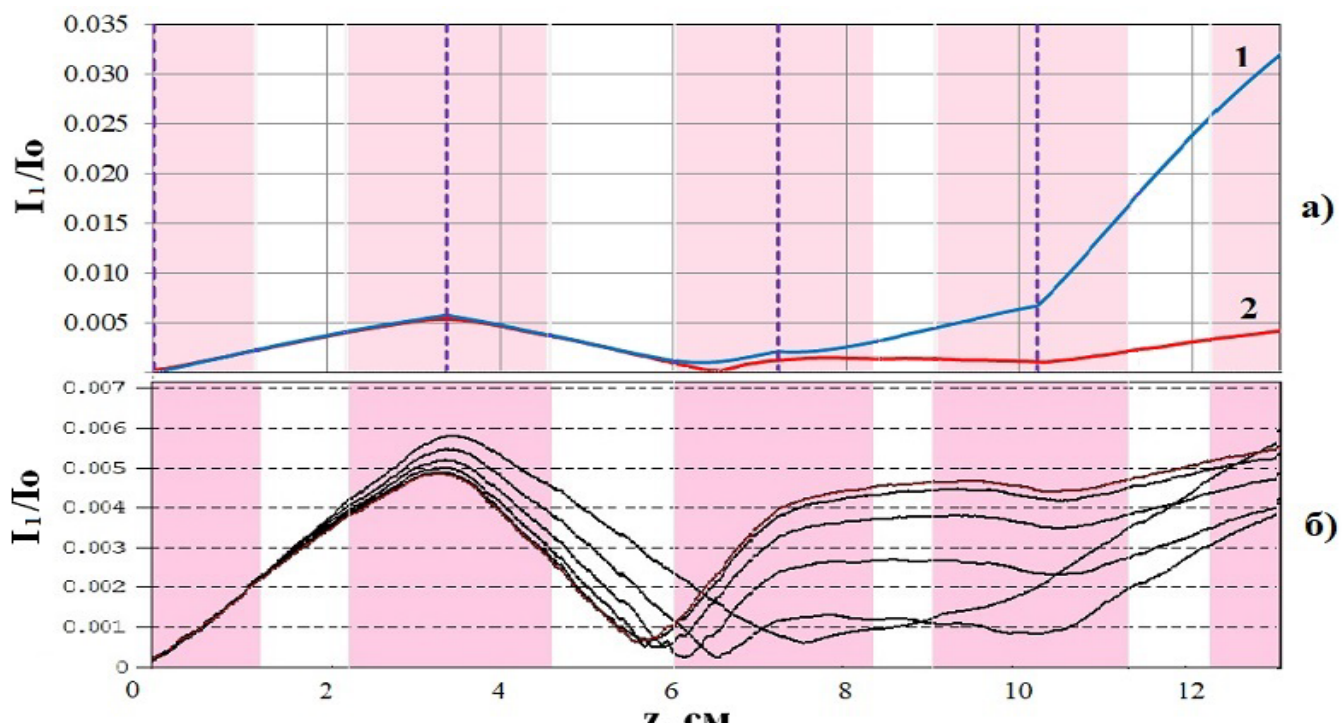


Fig. 3.

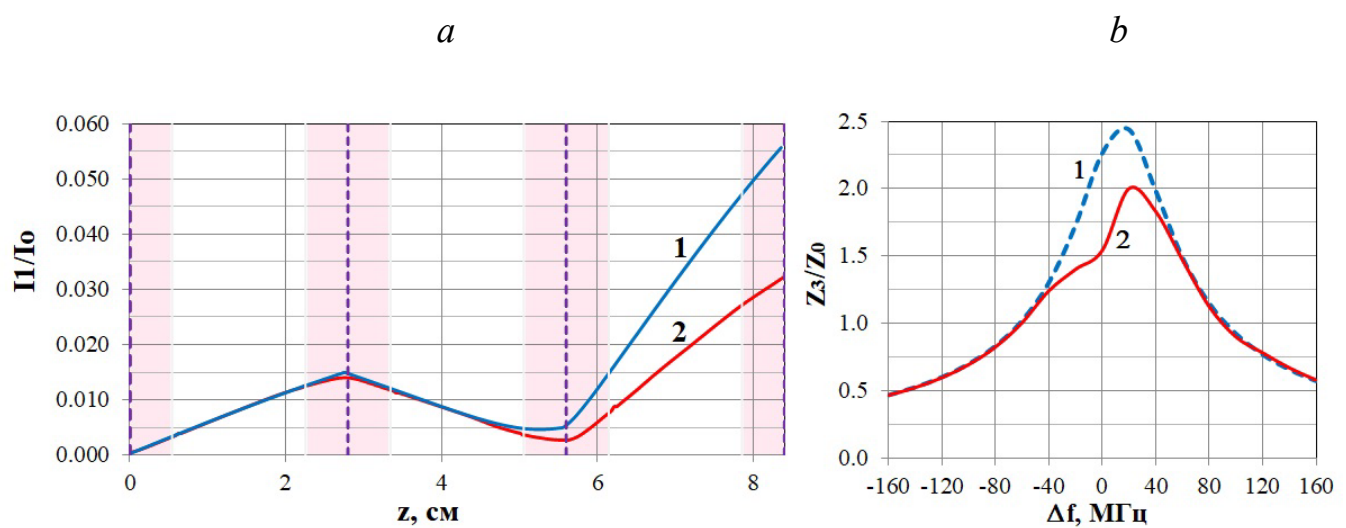


Fig. 4.